

Direction finding and mutual coupling estimation for uniform rectangular arrays



Han Wu^a, Chunping Hou^a, Hua Chen^a, Wei Liu^{b,*}, Qing Wang^a

^a School of Electronic Information Engineering, Tianjin University, Tianjin 300072, PR China

^b Department of Electronic and Electrical Engineering, University of Sheffield, Sheffield S1 3JD, UK

ARTICLE INFO

Article history:

Received 8 February 2015

Received in revised form

20 April 2015

Accepted 23 April 2015

Available online 1 May 2015

Keywords:

Direction of arrival estimation

Mutual coupling

Uniform rectangular array

Rank-reduction

ABSTRACT

A novel two-dimensional (2-D) direct-of-arrival (DOA) and mutual coupling coefficients estimation algorithm for uniform rectangular arrays (URAs) is proposed. A general mutual coupling model is first built based on banded symmetric Toeplitz matrices, and then it is proved that the steering vector of a URA in the presence of mutual coupling has a similar form to that of a uniform linear array (ULA). The 2-D DOA estimation problem can be solved using the rank-reduction method. With the obtained DOA information, we can further estimate the mutual coupling coefficients. A better performance is achieved by our proposed algorithm than those auxiliary sensor-based ones, as verified by simulation results.

© 2015 Elsevier B.V. All rights reserved.

1. Introduction

Direction of arrival (DOA) estimation for two-dimensional (2-D) arrays is an important area of array signal processing and has received much attention in past years [1]. The well-known multiple signal classification (MUSIC) algorithm can be applied directly for 2-D estimation [2], but its computational complexity is very high due to the required 2-D spectral search. On the other hand, the UCA-ESPRIT and 2-D Unitary ESPRIT algorithms can pair the azimuth and elevation angles belonging to the same source automatically without 2-D spectral searching or iterative optimization procedures [3,4]. In [5], a polynomial root-finding-based method was proposed using two parallel ULAs, by decoupling the 2-D problem into two 1-D problems to reduce the computational complexity. Another computationally efficient method was proposed in [6], where the propagator method in [7] was employed based on two parallel ULAs. However, this method requires pair matching between the 2-D azimuth and elevation estimation

results and may not work effectively for some situations. To overcome the problem in [6], an L-shaped array was employed instead in [8]. Based on such an L-shaped geometry, a 1-D searching algorithm without the need of pair matching was proposed in [9], while the subspace-based algorithm in [10] requires neither constructing the correlation matrix of the received data nor performing singular value decomposition (SVD) of the correlation matrix and utilizes the conjugate symmetry property to enlarge the effective array aperture. Another computationally efficient algorithm for URA was proposed in [11], where the complex-valued covariance matrix and the complex-valued search vector are transformed into real-valued ones, and the 2-D problem is decoupled into two 1-D problems with real-valued computations.

However, for the above algorithms and methods to work, it is normally assumed that the exact array manifold is known in advance, which may not be practical in many applications due to the effect of mutual coupling. Similar to the 1-D case, the effect of unknown mutual coupling can cause severe performance degradation in 2-D DOA estimation [12,13]. As a result, some 2-D array calibration algorithms have been proposed. In [14], azimuth estimation is decoupled from elevation estimation and can be performed

* Corresponding author.

E-mail addresses: dkchenhua@tju.edu.cn (H. Chen), w.liu@sheffield.ac.uk (W. Liu), wqelaine@tju.edu.cn (Q. Wang).

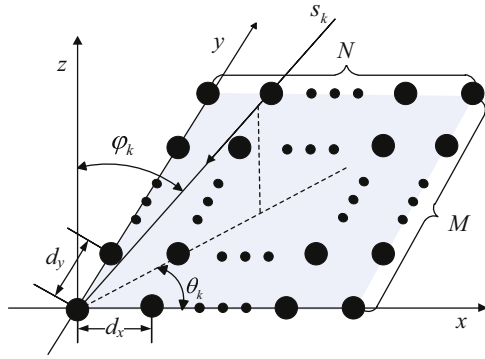


Fig. 1. Geometry of a URA with $M \times N$ sensors.

without the knowledge of mutual coupling, while for elevation estimation, a 1-D parameter search is performed and the elevation-dependent mutual coupling effect can be compensated effectively. In [15], a rank-reduction (RARE) algorithm for UCA was proposed based on the special structure of the coupling matrix considered in [16] and the result derived in [17]. In [18], two mutual coupling calibration methods were provided for uniform hexagon arrays (UHAs), one of which is also based on the method in [16], while the other is implemented by setting some auxiliary sensors. In [19], the mutual coupling model was extended to L-shaped arrays, where the mutual coupling effect is compensated using the outputs of properly chosen sensors and a rank-reduction propagator method is developed for joint estimation of both azimuth and elevation angles to avoid parameter pairing and 2D spectral search. To mitigate the effect of mutual coupling, the algorithm in [20] set the sensors on the array boundary to be auxiliary ones. The subarray's output and size are used to calculate the noise subspace and steering vector. The procedure of this algorithm is similar to the 2-D MUSIC algorithm. It obtains the DOAs through 2-D spectral searching by exploiting the orthogonality between the noise subspace and steering vector.

The auxiliary sensor-based algorithms, although effective in the presence of mutual coupling, share the common drawback that the effective aperture of the array is reduced. When considering mutual coupling between sensors farther apart, a larger number of auxiliary sensors are needed, which in turn reduces the number of sensors available for DOA estimation, since the total number of sensors is fixed. Therefore, the performance of these algorithms will deteriorate significantly when the size of original array is small or the mutual coupling effect is strong.

In this paper, we construct a general mutual coupling model for URAs using banded symmetric Toeplitz matrices and based on this model, we prove that the steering vector of such a URA in the presence of mutual coupling has a similar form to that of ULA using the method proposed in [21]; then, the rank-reduction method is introduced to estimate the azimuth and elevation angles, which are then used to obtain the unknown mutual coupling coefficients. As shown in our simulation results, the proposed

algorithm can achieve a better performance than auxiliary sensor-based ones since it employs the full array aperture for DOA estimation.

The rest of this paper is organized as follows. In Section 2, the signal model in the presence of mutual coupling is introduced. The proposed DOA and mutual coupling coefficients estimation algorithm is presented with detailed analysis of the steering vector in Section 3. Simulation results are given in Section 4 and conclusions are drawn in Section 5.

Notations: $(\cdot)^T$, $(\cdot)^H$ and $(\cdot)^+$ represent transpose, conjugate transpose and pseudo-inverse of a matrix or vector, respectively. $[\cdot]_{p,q}$ denotes the element at p th row and q th column of a matrix, and \otimes denotes the Kronecker product.

2. Problem formulation with banded symmetric Toeplitz mutual coupling matrix

Consider K far-field narrowband signals $s_k(t)$, $k = 1, 2, \dots, K$, with identical wavelength λ impinge on a URA of $M \times N$ omnidirectional sensors spaced by d_x in the x -axis direction and d_y in the y -axis direction, as shown in Fig. 1. The direction of arrival of the k th signal is denoted by (θ_k, φ_k) , where θ_k and φ_k are the azimuth and elevation angles, respectively. The received data vector $\mathbf{x}(t)$ of the array at sample t can be expressed as

$$\mathbf{x}(t) = \mathbf{A}\mathbf{s}(t) + \mathbf{n}(t) \quad (1)$$

where $\mathbf{x}(t) = [x_1(t), \dots, x_N(t), x_{N+1}(t), \dots, x_{2N}(t), \dots, x_{MN}(t)]^T$ holding the MN received array signals, $\mathbf{A} = [\mathbf{a}(\theta_1, \varphi_1), \mathbf{a}(\theta_2, \varphi_2), \dots, \mathbf{a}(\theta_K, \varphi_K)]^T$ is the array manifold matrix, $\mathbf{s}(t) = [s_1(t), s_2(t), \dots, s_K(t)]^T$ is the source signal vector and $\mathbf{n}(t) = [n_1(t), \dots, n_N(t), n_{N+1}(t), \dots, n_{2N}(t), \dots, n_{MN}(t)]^T$ is the additive white Gaussian noise vector. The steering vector $\mathbf{a}(\theta_k, \varphi_k)$ can be modeled as

$$\mathbf{a}(\theta_k, \varphi_k) = \mathbf{a}_y(\theta_k, \varphi_k) \otimes \mathbf{a}_x(\theta_k, \varphi_k) \quad (2)$$

where

$$\mathbf{a}_y(\theta_k, \varphi_k) = [1, \beta_y(\theta_k, \varphi_k), \dots, \beta_y^{M-1}(\theta_k, \varphi_k)]^T \quad (3)$$

$$\mathbf{a}_x(\theta_k, \varphi_k) = [1, \beta_x(\theta_k, \varphi_k), \dots, \beta_x^{N-1}(\theta_k, \varphi_k)]^T \quad (4)$$

with

$$\beta_y(\theta_k, \varphi_k) = \exp\{j2\pi\lambda^{-1}d_y \sin(\theta_k) \sin(\varphi_k)\} \quad (5)$$

$$\beta_x(\theta_k, \varphi_k) = \exp\{j2\pi\lambda^{-1}d_x \cos(\theta_k) \sin(\varphi_k)\} \quad (6)$$

For simplified notation, the pair of angles (θ, φ) is omitted in the following when not causing any confusion.

Considering the effect of mutual coupling, (1) should be modified as

$$\mathbf{x}(t) = \mathbf{C}\mathbf{A}\mathbf{s}(t) + \mathbf{n}(t) \quad (7)$$

where \mathbf{C} denotes the mutual coupling matrix (MCM). As indicated in [16,20,22], the coupling between neighboring sensors with the same inter-element spacing is almost the same, while the magnitude of mutual coupling coefficients between two far apart elements would be so small that this effect can be ignored. Therefore, the mutual coupling of ULA can be modeled as a banded symmetric Toeplitz matrix. In [20], this model was extended to URAs assuming that each sensor is only affected by the 8 immediately

surrounding sensors, and no general mutual coupling model is given. In this section, we will build a general mutual coupling model for URAs. First, we define a parameter P as mutual coupling length for URA, which means for each sensor, we only consider the mutual coupling effect caused by sensors on the 1st, 2nd, ..., $(P-1)$ th rectangular grid around it. This definition is illustrated in Fig. 2 with $P=n+1$. Then the MCM can be expressed as a block matrix

$$\mathbf{C} = \begin{bmatrix} \mathbf{C}_1 & \mathbf{C}_2 & \cdots & \mathbf{C}_P \\ \mathbf{C}_2 & \mathbf{C}_1 & \mathbf{C}_2 & \ddots & \ddots \\ \vdots & \ddots & \ddots & \ddots & \ddots \\ \mathbf{C}_P & \mathbf{C}_2 & \mathbf{C}_1 & \mathbf{C}_2 & \mathbf{C}_P \\ & \ddots & & \ddots & \vdots \\ & & \ddots & \mathbf{C}_2 & \mathbf{C}_1 & \mathbf{C}_2 \\ & & & \mathbf{C}_P & \cdots & \mathbf{C}_2 & \mathbf{C}_1 \end{bmatrix} \quad (8)$$

where \mathbf{C} is an $MN \times MN$ matrix and \mathbf{C}_i ($i=1, 2, \dots, P$) are $N \times N$ sub-matrices, where

$$\mathbf{C}_i = \begin{bmatrix} c_{i-1,0} & c_{i-1,1} & \cdots & c_{i-1,P-1} \\ c_{i-1,1} & c_{i-1,0} & c_{i-1,1} & \ddots \\ \vdots & c_{i-1,1} & c_{i-1,0} & \ddots & c_{i-1,P-1} \\ c_{i-1,P-1} & \ddots & \ddots & c_{i-1,1} & \vdots \\ & & c_{i-1,P-1} & \cdots & c_{i-1,1} & c_{i-1,0} \end{bmatrix} \quad (9)$$

The coefficients c_{ij} denote the mutual coupling from the sensor located at $(\pm i, \pm j)$, $i \neq 0, j \neq 0$ where $(\pm i, \pm j)$ denotes the coordinate of the sensor in Fig. 2. Especially, we define $c_{0,0} = 1$.

The covariance matrix of $\mathbf{x}(t)$ is

$$\mathbf{R}_x = E[\mathbf{x}(t)\mathbf{x}^H(t)] = \mathbf{C}\mathbf{R}_s\mathbf{A}^H\mathbf{C}^H + \sigma^2\mathbf{I} \quad (10)$$

where $\mathbf{R}_s = E[\mathbf{s}(t)\mathbf{s}^H(t)]$ is the signal covariance matrix. In practice, \mathbf{R}_x can be approximated by

$$\mathbf{R}_x \approx \frac{1}{L} \sum_{t=1}^L \mathbf{x}(t)\mathbf{x}^H(t) \quad (11)$$

where L is the number of data snapshots available. Then

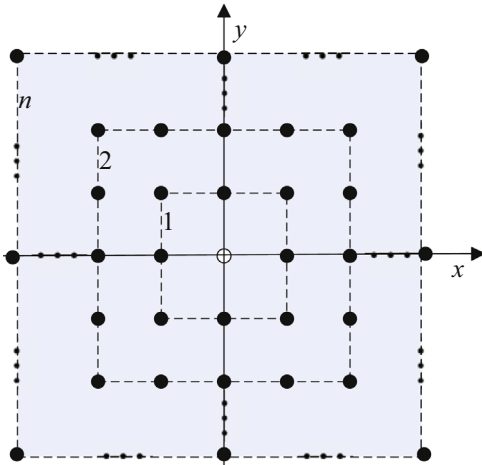


Fig. 2. The mutual coupling model for URAs with $P=n+1$.

the eigendecomposition of \mathbf{R}_x is

$$\mathbf{R}_x = \mathbf{E}_s \Sigma_s \mathbf{E}_s^H + \mathbf{E}_n \Sigma_n \mathbf{E}_n^H \quad (12)$$

where \mathbf{E}_s and \mathbf{E}_n are the signal subspace and noise subspace, respectively. $\Sigma_s = \text{diag}(\lambda_1, \lambda_2, \dots, \lambda_K)$ and $\Sigma_n = \text{diag}(\lambda_{K+1}, \lambda_{K+2}, \dots, \lambda_{MN})$ are diagonal matrices, with $\lambda_1 \geq \lambda_2 \geq \dots \geq \lambda_K > \lambda_{K+1} = \dots = \lambda_{MN} = \sigma^2$ being the corresponding eigenvalues of \mathbf{R}_x .

3. The proposed algorithm

Since the MCM of a URA and its submatrices share the same structure of banded symmetric Toeplitz matrix, the parameterization method for the steering vector, which was originally proposed in [21] for a ULA, can be extended to the URA case.

The steering vector of the URA with mutual coupling is given by

$$\mathbf{a}_c = \mathbf{C}\mathbf{a} \quad (13)$$

It is difficult to find the exact form of \mathbf{a}_c from (13) since \mathbf{C} is a block matrix. So we first decompose \mathbf{C} into the following form:

$$\mathbf{C} = \mathbf{I}_M \otimes \mathbf{C}_1 + \sum_{i=2}^P \mathbf{J}_{i-1} \otimes \mathbf{C}_i \quad (14)$$

where \mathbf{I}_M is an $M \times M$ identity matrix. \mathbf{J}_{i-1} is an $M \times M$ matrix, whose elements are

$$[\mathbf{J}_{i-1}]_{p,q} = \begin{cases} 1, & |p-q| = i-1 \\ 0 & \text{otherwise} \end{cases} \quad (15)$$

Substituting (2) and (14) into (13), the steering vector can now be expressed as

$$\begin{aligned} \mathbf{a}_c &= \left(\mathbf{I}_M \otimes \mathbf{C}_1 + \sum_{i=2}^P \mathbf{J}_{i-1} \otimes \mathbf{C}_i \right) (\mathbf{a}_y \otimes \mathbf{a}_x) \\ &= (\mathbf{I}_M \otimes \mathbf{C}_1) (\mathbf{a}_y \otimes \mathbf{a}_x) + \left(\sum_{i=2}^P \mathbf{J}_{i-1} \otimes \mathbf{C}_i \right) (\mathbf{a}_y \otimes \mathbf{a}_x) \\ &= \mathbf{I}_M \mathbf{a}_y \otimes \mathbf{C}_1 \mathbf{a}_x + \sum_{i=2}^P (\mathbf{J}_{i-1} \mathbf{a}_y \otimes \mathbf{C}_i \mathbf{a}_x) \end{aligned} \quad (16)$$

Note that \mathbf{a}_x and \mathbf{a}_y have exactly the same form as the steering vector of a ULA, and \mathbf{C}_i ($i=1, 2, \dots, P$) also the same form as the MCM of a ULA. Moreover, \mathbf{I}_M and \mathbf{J}_{i-1} can be regarded as special cases of \mathbf{C}_i .

According to [21], we can express $\mathbf{C}_i \mathbf{a}_x$ as

$$\mathbf{C}_i \mathbf{a}_x = \mathbf{T}_x \alpha_{xi} \quad (17)$$

where

$$\mathbf{T}_x = \begin{bmatrix} 1 & & & & & & 0 \\ & \beta_x & & & & & \\ & & \ddots & & & & \\ & & & \beta_x^{P-1} & & & \\ & & & \vdots & & & \\ & & & \beta_x^{N-P} & & & \\ 0 & & & & \ddots & & \\ & & & & & \beta_x^{N-1} & \end{bmatrix} \quad (18)$$

and $\alpha_{x,i}$ ($i = 1, 2, \dots, P$) is a $(2P-1)$ -element column vector related to mutual coupling coefficients:

$$\alpha_{x,i} = \begin{bmatrix} \xi_{1,i} \\ \vdots \\ \xi_{P-1,i} \\ c_{i-1,0} + \sum_{l=1}^{P-1} c_{i-1,l} (\beta_x^l + \beta_x^{-l}) \\ \mu_{1,i} \\ \vdots \\ \mu_{P-1,i} \end{bmatrix} \quad (19)$$

where $\xi_{n,i} = c_{i-1,0} + \sum_{l=1}^{n-1} c_{i-1,l} \beta_x^{-l} + \sum_{l=1}^{P-1} c_{i-1,l} \beta_x^l$ and

$$\mu_{n,i} = c_{i-1,0} + \sum_{l=1}^{P-1} c_{i-1,l} \beta_x^{-l} + \sum_{l=1}^{P-1-n} c_{i-1,l} \beta_x^l$$

($n = 1, 2, \dots, P-1$).

Define η_n as an n -element column vector of ones

$$\eta_n = \begin{bmatrix} 1, 1, \dots, 1, 1 \end{bmatrix}^T \quad (20)$$

When $i = 1$

$$\alpha_{x,1} = \eta_{2P-1} + \mathbf{F}' \mathbf{c}'_0 \quad (21)$$

where

$$[\mathbf{F}']_{p,q} = \begin{cases} \beta_x^{-q} + \beta_x^q, & q+1 \leq p \leq 2P-q-1 \\ \beta_x^q, & p < q+1 \\ \beta_x^{-q}, & p > 2P-q-1 \end{cases} \quad (22)$$

$$\mathbf{c}'_0 = [c_{0,1}, c_{0,2}, \dots, c_{0,P-1}]^T \quad (23)$$

When $i > 1$

$$\alpha_{x,i} = \mathbf{F} \mathbf{c}_{i-1} \quad (24)$$

where

$$\mathbf{F} = [\eta_{2P-1}, \mathbf{F}'] \quad (25)$$

$$\mathbf{c}_{i-1} = [c_{i-1,0}, c_{i-1,1}, \dots, c_{i-1,P-1}]^T \quad (26)$$

Similar to (17), we also have

$$\mathbf{I}_M \mathbf{a}_y = \mathbf{T}_y \alpha_{y,1} \quad (27)$$

$$\mathbf{J}_{i-1} \mathbf{a}_y = \mathbf{T}_y \alpha_{y,i} \quad (28)$$

where

$$\mathbf{T}_y = \begin{bmatrix} 1 & & & & & \\ & \beta_y & & & & \\ & & \ddots & & & \\ & & & \beta_y^{P-1} & & \\ & & & \vdots & & \\ & & & \beta_y^{M-P} & & \\ & & & & \ddots & \\ \mathbf{0} & & & & & \beta_y^{M-1} \end{bmatrix} \quad (29)$$

and $\alpha_{y,i}$ ($i = 1, 2, \dots, P$) is a $(2P-1)$ -element column vector independent of the mutual coupling coefficients. When $i = 1$

$$\alpha_{y,1} = \eta_{2P-1} \quad (30)$$

When $i > 1$, the p th element of $\alpha_{y,i}$ is

$$[\alpha_{y,i}]_p = \begin{cases} \beta_y^{-(i-1)} + \beta_y^{i-1}, & i \leq p \leq 2P-i \\ \beta_y^{i-1}, & p < i \\ \beta_y^{-(i-1)}, & p > 2P-i \end{cases} \quad (31)$$

Substituting (17), (27) and (28), (16) can be further modified as

$$\begin{aligned} \mathbf{a}_c &= \mathbf{T}_y \alpha_{y,1} \otimes \mathbf{T}_x \alpha_{x,1} + \sum_{i=2}^P (\mathbf{T}_y \alpha_{y,i} \otimes \mathbf{T}_x \alpha_{x,i}) \\ &= (\mathbf{T}_y \otimes \mathbf{T}_x) (\alpha_{y,1} \otimes \alpha_{x,1}) + \sum_{i=2}^P (\mathbf{T}_y \otimes \mathbf{T}_x) (\alpha_{y,i} \otimes \alpha_{x,i}) \\ &= \mathbf{T} \alpha_1 + \sum_{i=2}^P \mathbf{T} \alpha_i \\ &= \mathbf{T} \alpha \end{aligned} \quad (32)$$

where

$$\mathbf{T} = \mathbf{T}_y \otimes \mathbf{T}_x, \alpha_i = \alpha_{y,i} \otimes \alpha_{x,i} (i = 1, 2, \dots, P), \alpha = \alpha_1 + \sum_{i=2}^P \alpha_i$$

Now we can see that the steering vector of a URA in the presence of mutual coupling has a similar form as that of a ULA, which indicates that the DOA estimation methods developed in [21] based on ULAs can be extended to the URA case. In the next subsections we will show how to perform this extension and also use the estimated DOA information to obtain the mutual coupling coefficients.

3.1. DOA estimation

According to the subspace principle, the noise subspace is orthogonal to the steering vectors, i.e.

$$\mathbf{a}_c^H \mathbf{E}_n \mathbf{E}_n^H \mathbf{a}_c = 0. \quad (33)$$

From (32), we have derived the result $\mathbf{a}_c = \mathbf{T} \alpha$. Then substituting it into (33), we can obtain the following result directly:

$$\alpha^H \mathbf{T}^H \mathbf{E}_n \mathbf{E}_n^H \mathbf{T} \alpha = 0. \quad (34)$$

Now define a $(2P-1) \times (2P-1)$ matrix $\mathbf{M}(\theta, \varphi)$

$$\mathbf{M}(\theta, \varphi) \triangleq \mathbf{T}^H \mathbf{E}_n \mathbf{E}_n^H \mathbf{T} \quad (35)$$

Note that if

$$(2P-1)^2 \leq MN - K \quad (36)$$

then, in general, $\mathbf{M}(\theta, \varphi)$ is of full rank because in this case, the column rank of \mathbf{E}_n is not less than $(2P-1)^2$. Therefore, (34) holds true only if $\mathbf{M}(\theta, \varphi)$ drops rank so that

$$\text{rank}\{\mathbf{M}(\theta, \varphi)\} < (2P-1)^2 \quad (37)$$

Since the covariance matrix of $\mathbf{x}(t)$ is obtained from a finite number of samples, the reduction of the rank of $\mathbf{M}(\theta, \varphi)$ can roughly be replaced by the minimum of the determinant of $\mathbf{M}(\theta, \varphi)$, which indicates that (θ, φ) coincides with one of the signal's DOAs, i.e., $(\theta, \varphi) = (\theta_k, \varphi_k), k = 1, 2, \dots, K$. Therefore, the DOA estimation results can be found from the K highest peaks of the following function:

$$P(\theta, \varphi) = \frac{1}{\det\{\mathbf{M}(\theta, \varphi)\}}, \quad (38)$$

where $\det\{\cdot\}$ denotes the determinant of a matrix.

3.2. Mutual coupling coefficients estimation

With the estimated DOA information from (38), we can then proceed to estimate the mutual coupling coefficients. Using the k th pair of estimated DOAs, i.e., $(\hat{\theta}_k, \hat{\varphi}_k)$, we have

$$\mathbf{E}_n^H \mathbf{T}(\hat{\theta}_k, \hat{\varphi}_k) \boldsymbol{\alpha}(\hat{\theta}_k, \hat{\varphi}_k) = \mathbf{0}. \quad (39)$$

From (21), (24), (30), $\boldsymbol{\alpha}$ can be expressed as

$$\boldsymbol{\alpha} = \boldsymbol{\eta}_{(2P-1)^2} + \boldsymbol{\eta}_{2P-1} \otimes \mathbf{F}' \mathbf{c}'_0 + \sum_{i=2}^P \boldsymbol{\alpha}_{y,i} \otimes \mathbf{F} \mathbf{c}_{i-1} \quad (40)$$

or

$$\boldsymbol{\alpha} = \boldsymbol{\eta}_{(2P-1)^2} + \mathbf{G} \mathbf{c} \quad (41)$$

where

$$\mathbf{G} = [\boldsymbol{\eta}_{2P-1} \otimes \mathbf{F}', [\boldsymbol{\alpha}_{y,2}, \dots, \boldsymbol{\alpha}_{y,P}] \otimes \mathbf{F}] \quad (42)$$

$$\mathbf{c} = [\mathbf{c}'_0, \mathbf{c}_1, \dots, \mathbf{c}_{P-1}]^T \quad (43)$$

Substituting (41) into (39)

$$\mathbf{E}_n^H \mathbf{T}(\boldsymbol{\eta}_{(2P-1)^2} + \mathbf{G} \mathbf{c}) = \mathbf{0} \quad (44)$$

Define $\mathbf{F} \triangleq \mathbf{E}_n^H \mathbf{T} \mathbf{G}$, $\mathbf{Z} \triangleq -\mathbf{E}_n^H \mathbf{T} \boldsymbol{\eta}_{(2P-1)^2}$ and construct two matrices $\bar{\mathbf{F}} \triangleq [\mathbf{F}_1^T, \mathbf{F}_2^T, \dots, \mathbf{F}_K^T]^T$ and $\bar{\mathbf{Z}} \triangleq [\mathbf{Z}_1^T, \mathbf{Z}_2^T, \dots, \mathbf{Z}_K^T]^T$, where \mathbf{F}_k and \mathbf{Z}_k denote the \mathbf{F} and \mathbf{Z} obtained using the k th pair of estimated DOAs. Then the unknown mutual coupling coefficients can be obtained by

$$\mathbf{c} = \bar{\mathbf{F}}^+ \bar{\mathbf{Z}}. \quad (45)$$

Now the paired angle parameter $(\hat{\theta}_k, \hat{\varphi}_k)$ as well as the mutual coupling coefficients have been estimated. The proposed algorithm mentioned above is summarized with the flow chart shown in Fig. 3.

3.3. Computational complexity analysis

To estimate the sample covariance matrix, a computational complexity of $O((MN)^2 L)$ is needed. The eigendecomposition operation has a computational complexity of $O((MN)^3)$. For 2-D spectral searching, at each DOA sampling point, the matrix \mathbf{T} , \mathbf{M} , and $\det\{\mathbf{M}\}$ should be calculated, which are associated with a complexity of $O(MN)$, $O(MN(MN-K)(2P-1)^2 + (MN-K)(2P-1)^4)$, and $O((MN)^3)$, respectively. Therefore, the complexity for the whole 2-D spectral searching process is $O(n(MN + MN(MN-K)(2P-1)^2 + (MN-K)(2P-1)^4 + (MN)^3))$, where $n = (360^\circ/\Delta)^2$ is the number of sampling points, with Δ being the scanning interval, which is also the accuracy of estimated angles. As an example, for $\Delta = 0.1^\circ$, we have $n = 3600^2$. To reduce the computational complexity, we have adopted the two-level searching method in [20] in our simulations. In the first round of searching, we find each pair of angles (θ_k, φ_k) with an interval of $\Delta = 1^\circ$. In the second round, we search in the range of $(\theta_k - 1^\circ, \varphi_k - 1^\circ)$ to $(\theta_k + 1^\circ, \varphi_k + 1^\circ)$ with an interval of 0.1° . As a result, the number of sampling points is reduced significantly without affecting much of the estimation accuracy.

Now we analyze the complexity for mutual coupling estimation. To obtain $\bar{\mathbf{F}}$ and $\bar{\mathbf{Z}}$, the total

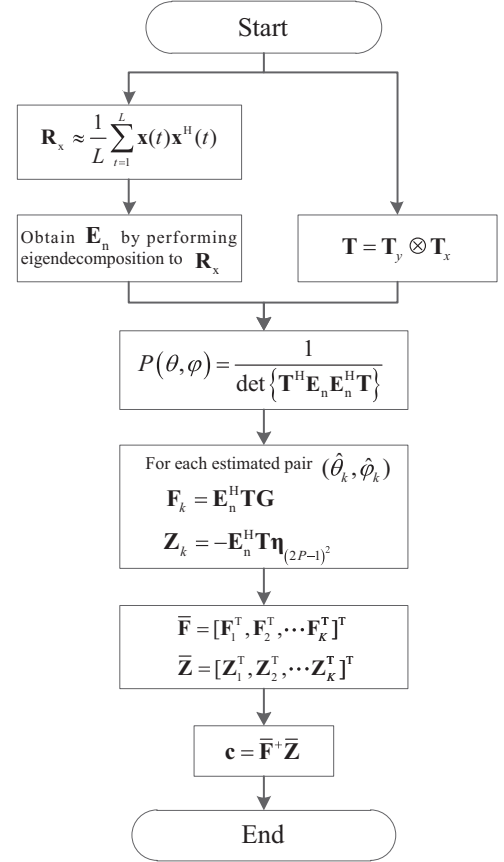


Fig. 3. The flow chart of the proposed algorithm.

computational complexity is $O(K(MN(MN-K)(2P-1)^2 + (MN-K)(2P-1)^3))$. The pseudo-inverse of $\bar{\mathbf{F}}$ costs $O(K^3(MN-K)^3)$. It needs $O(K(MN-K)(2P-1))$ to calculate the coefficients in the last step.

4. Simulation results

In this section, simulation results are provided to demonstrate the performance of the proposed algorithm. For all simulations, 4 uncorrelated signals with the same frequency and power of σ_s^2 from the directions $(\theta_1 = 28^\circ, \varphi_1 = 41^\circ)$, $(\theta_2 = 40^\circ, \varphi_2 = 20^\circ)$, $(\theta_3 = 54^\circ, \varphi_3 = 66^\circ)$ and $(\theta_4 = 74^\circ, \varphi_4 = 35^\circ)$ are considered. The URA has $M = 10$ rows and $N = 10$ columns. Both d_x and d_y are half wavelength. The power of additive white Gaussian noise is σ_n^2 and the signal-to-noise ratio (SNR) is defined as $\text{SNR} = 10 \log_{10}(\sigma_s^2/\sigma_n^2)$. We use root mean square error (RMSE) to evaluate the effectiveness of our algorithm and 100 Monte Carlo simulations are performed to obtain the averaged result. The RMSE of estimated angles is defined as

$$\text{RMSE} = \sqrt{\frac{1}{N_{mc} K} \sum_{i=1}^{N_{mc}} \sum_{k=1}^K |(\hat{\theta}_{ik}, \hat{\varphi}_{ik}) - (\theta_k, \varphi_k)|^2} \quad (46)$$

where N_{mc} denotes the number of Monte Carlo simulations, and $(\hat{\theta}_{ik}, \hat{\varphi}_{ik})$ is the estimated (θ_k, φ_k) in the i th Monte Carlo simulation. The RMSE of estimated coefficients is

defined as

$$\text{RMSE} = \sqrt{\frac{1}{N_{mc} \|\mathbf{c}\|_2^2} \sum_{i=1}^{N_{mc}} \|\hat{\mathbf{c}}_i - \mathbf{c}\|_2^2} \quad (47)$$

where \mathbf{c} is defined in (43), and $\hat{\mathbf{c}}_i$ is the estimated \mathbf{c} in the i th Monte Carlo simulation. $\|\cdot\|_2$ denotes the Euclidean norm.

In the first three sets of simulations, we set $P=2$, i.e. there are 3 mutual coupling coefficients to estimate and the following values are used $c_{0,1} = c_{1,0} = 0.3527 + 0.4854j$ and $c_{1,1} = 0.0927 - 0.2853j$.

4.1. Performance versus SNR

First, the performance of the proposed algorithm is studied with a varying SNR from -5 dB to 15 dB. The number of data samples is 500. The results are shown in Fig. 4, where for comparison, those obtained by the algorithm in [20], 2-D MUSIC with unknown mutual coupling, 2-D MUSIC with known mutual coupling, and CRB (Cramer–Rao bound) in [20] are also provided.

It can be seen that the 2-D MUSIC with known mutual coupling provides the best result, while our proposed algorithm has reached a better result than the one in [20]. As expected, the 2-D MUSIC with unknown mutual coupling does not work in this context. The RMSE curve of the estimated mutual coupling coefficients is shown in Fig. 5, where the algorithm in [20] and our proposed one have an almost identical performance and both have worked effectively.

4.2. Performance versus snapshots

In this set of simulations, we fix the SNR to 0 dB and study the performance of the algorithms with a varying snapshot number from 100 to 1000. The RMSE result for angle estimation is shown in Fig. 6, while the result for mutual coupling coefficients estimation is shown in Fig. 7. Similar observations can be made as in the varying SNR case in Section 4.1. Our proposed algorithm has a better

performance than the one in [20] for DOA estimation and almost the same performance for mutual coupling coefficients estimation.

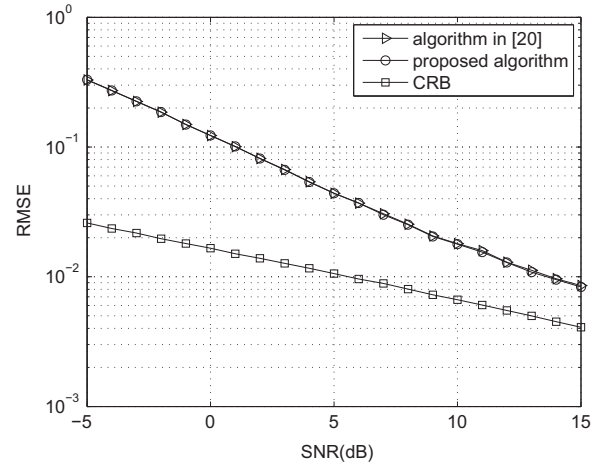


Fig. 5. RMSE of estimated mutual coupling coefficients versus SNR.

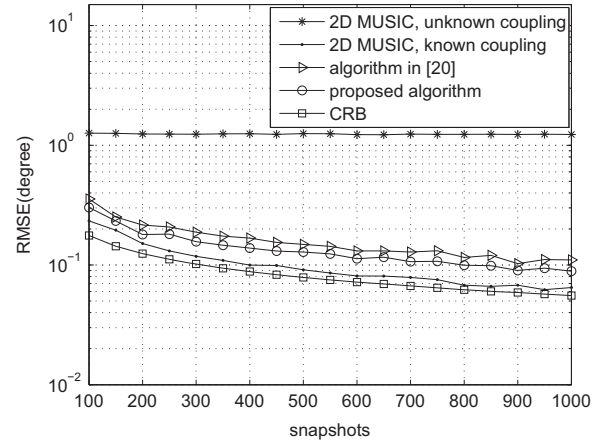


Fig. 6. RMSE of estimated angles versus snapshots.

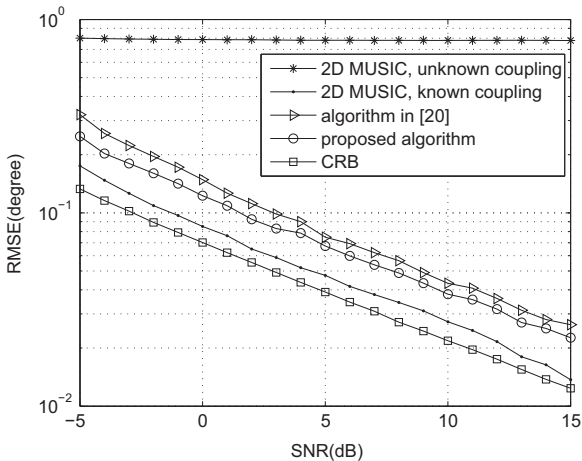


Fig. 4. RMSE of estimated angles versus SNR.

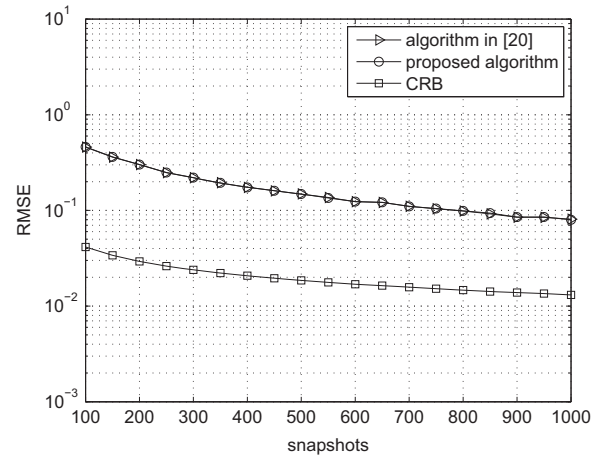


Fig. 7. RMSE of estimated mutual coupling coefficients versus snapshots.

4.3. Performance versus size of array

Now we study the effect of array size change on the performance. M and N are assigned the same value and vary from 6 to 15. The SNR is fixed at 0 dB and the number of snapshot is 500. Fig. 8 shows the RMSE of estimated angles obtained by the algorithm in [20] and the proposed one. It can be seen that the superiority of our proposed algorithm is more significant when the size of array is small.

4.4. Performance under strong mutual coupling

Finally, we consider a scenario with strong mutual coupling and the length is chosen to be $P=3$, i.e. each sensor is affected by 24 surrounding sensors and eight mutual coupling coefficients are needed, which are $c_{0,1} = c_{1,0} = 0.7527 + 0.4854j$, $c_{1,1} = 0.5211 + 0.3250j$, $c_{0,2} = c_{2,0} = 0.2825 + 0.2801j$, $c_{1,2} = c_{2,1} = 0.1477 + 0.1475j$, $c_{2,2} = 0.0927 - 0.1253j$. The SNR varies from 0 dB to 15 dB and the number of snapshots is 500. The results are shown in Figs. 9 and 10. Comparing Figs. 9 and 10 with Figs. 4 and 5, respectively, we can see that the improvement in angle estimation by our proposed algorithm is much larger, while for mutual coupling coefficients estimation, it is now clearly visible.

4.5. The running time comparison

All the simulations in this paper are performed by MATLAB 7.8.0 on a personal computer with Intel Core i5 760 CPU and 2 GB memory. As an indicator of the computational complexity of the algorithms, the running time for each algorithm studied in the first set of simulations is provided in Table 1. We can see that the proposed algorithm has the longest running time. However, it is still comparable to the algorithm in [20] and the 2-D MUSIC.

5. Conclusion

In this paper, a novel 2-D DOA and mutual coupling coefficients estimation algorithm for URAs has been proposed.

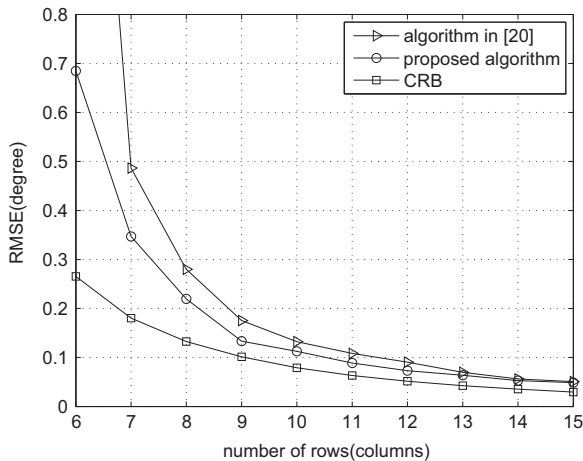


Fig. 8. RMSE of estimated angles versus number of rows (columns).

We started by creating a general mutual coupling model based on banded symmetric Toeplitz matrices, and then proved that the steering vector of a URA in the presence of mutual coupling has a similar form to that of a ULA. The 2-D DOA estimation problem can be solved using the rank-reduction method. Different from auxiliary sensor based algorithms, where the effective array aperture is reduced due to the use of auxiliary sensors, our proposed algorithm can keep the original array aperture and achieve a better performance in both DOA and mutual coupling coefficients estimation, especially when the array size is small or the mutual coupling effect is strong.

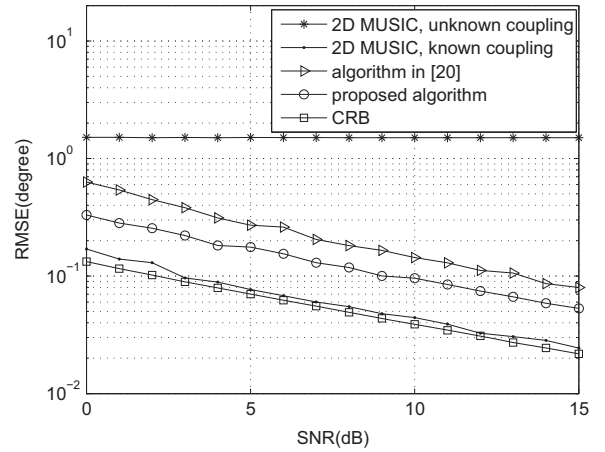


Fig. 9. RMSE of estimated angles versus SNR with $P=3$.

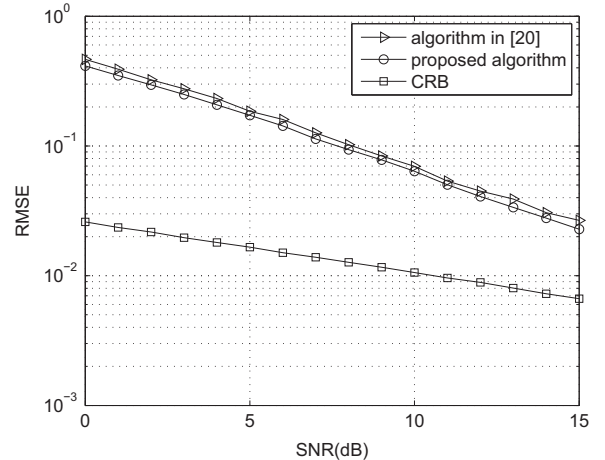


Fig. 10. RMSE of estimated mutual coupling coefficients versus SNR with $P=3$.

Table 1

The running time for each algorithm.

Proposed algorithm	Algorithm in [20]	2-D MUSIC
5771.1368 s	2320.5360 s	3074.9745 s

Acknowledgment

This work is supported by the National Natural Science Foundation of China under Grant (No. 61101223), and by Ph.D. Programs Foundation of Ministry of Education of China (Nos. 20110032120087 and 20110032110029).

References

- [1] H. Krim, M. Viberg, Two decades of array signal processing research: the parametric approach, *IEEE Signal Process. Mag.* 13 (4) (1996) 67–94.
- [2] R.O. Schmidt, Multiple emitter location and signal parameter estimation, *IEEE Trans. Antennas Propag.* 34 (3) (1986) 276–280.
- [3] C.P. Mathews, M.D. Zoltowski, Eigenstructure techniques for 2-D angle estimation with uniform circular arrays, *IEEE Trans. Signal Process.* 42 (9) (1994) 2395–2407.
- [4] M.D. Zoltowski, M. Haardt, C.P. Mathews, Closed-form 2-D angle estimation with rectangular arrays in element space or beamspace via unitary ESPRIT, *IEEE Trans. Signal Process.* 44 (2) (1996) 316–328.
- [5] T. Xia, Y. Zheng, Q. Wan, X. Wang, Decoupled estimation of 2-D angles of arrival using two parallel uniform linear arrays, *IEEE Trans. Antennas Propag.* 55 (9) (2007) 2627–2632.
- [6] Y. Wu, G. Liao, H.C. So, A fast algorithm for 2-D direction-of-arrival estimation, *Signal Process.* 83 (8) (2003) 1827–1831.
- [7] S. Marcos, A. Marsal, M. Benidir, The propagator method for source bearing estimation, *Signal Process.* 42 (2) (1995) 121–138.
- [8] N. Tayem, H.M. Kwon, L-shape 2-dimensional arrival angle estimation with propagator method, *IEEE Trans. Antennas Propag.* 53 (5) (2005) 1622–1630.
- [9] J. Liang, D. Liu, Joint elevation and azimuth direction finding using L-shaped array, *IEEE Trans. Antennas Propag.* 58 (6) (2010) 2136–2141.
- [10] X. Nie, L. Li, A computationally efficient subspace algorithm for 2-D DOA estimation with L-shaped array, *IEEE Signal Process. Lett.* 21 (8) (2014) 971–974.
- [11] W. Zhang, W. Liu, J. Wang, S. Wu, Computationally efficient 2-D DOA estimation for uniform rectangular arrays, *Multidimens. Syst. Signal Process.* 25 (4) (2014) 847–857.
- [12] C. Roller, W. Wasylkiwskyj, Effects of mutual coupling on super-resolution DF in linear arrays, in: *Proceedings of IEEE International Conference on Acoustics, Speech and Signal Processing*, vol. 5, 1992, pp. 257–260.
- [13] A.J. Weiss, B. Friedlander, Mutual coupling effects on phase-only direction finding, *IEEE Trans. Antennas Propag.* 40 (5) (1992) 535–541.
- [14] B.H. Wang, H.T. Hui, M.S. Leong, Decoupled 2D direction of arrival estimation using compact uniform circular arrays in the presence of elevation-dependent mutual coupling, *IEEE Trans. Antennas Propag.* 58 (3) (2010) 747–755.
- [15] J. Dai, X. Bao, N. Hu, C. Chang, W. Xu, A recursive RARE algorithm for DOA estimation with unknown mutual coupling, *IEEE Antennas Wirel. Propag. Lett.* 13 (2014) 1593–1596.
- [16] B. Friedlander, A.J. Weiss, Direction finding in the presence of mutual coupling, *IEEE Trans. Antennas Propag.* 39 (3) (1991) 273–284.
- [17] M. Pesavento, A.B. Gershman, K.M. Wong, Direction finding in partly calibrated sensor arrays composed of multiple subarrays, *IEEE Trans. Signal Process.* 50 (9) (2002) 2103–2115.
- [18] C. Liu, Z. Ye, Y. Zhang, Autocalibration algorithm for mutual coupling of planar array, *Signal Process.* 90 (3) (2010) 784–794.
- [19] J. Liang, X. Zeng, W. Wang, H. Chen, L-shaped array-based elevation and azimuth direction finding in the presence of mutual coupling, *Signal Process.* 91 (50) (2011) 1319–1328.
- [20] Z. Ye, C. Liu, 2-D DOA estimation in the presence of mutual coupling, *IEEE Trans. Antennas Propag.* 56 (10) (2008) 3150–3158.
- [21] B. Liao, Z.G. Zhang, S.C. Chan, DOA estimation and tracking of ULAs with mutual coupling, *IEEE Trans. Aerosp. Electron. Syst.* 48 (1) (2012) 891–905.
- [22] T. Svantesson, Modeling and estimation of mutual coupling in a uniform linear array of dipoles, in: *Proceedings of IEEE International Conference on Acoustics, Speech and Signal Processing*, vol. 5, 1999, pp. 2961–2964.